JOURNAL OF GUIDANCE, CONTROL, AND DYNAMICS
Vol. 39, No. 5, May 2016

Manual Control Adaptation to Changing Vehicle Dynamics in Roll–Pitch Control Tasks

Peter M.T. Zaal*
San Jose State University, NASA Ames Research Center, Moffett Field, California 94035

DOI: 10.2514/1.G001592

This paper investigates how pilot control behavior adapts to time-varying vehicle dynamics in a roll–pitch control task. Nine general aviation pilots performed eight experimental conditions in which the axis containing the time-varying controlled dynamics and the rate of change of the dynamics varied. To characterize time-varying human control behavior, a maximum likelihood estimation procedure was used to estimate the parameters of a pilot model with time-dependent sigmoid functions. Pilot control behavior in both axes was significantly affected by the time-varying controlled dynamics in roll and pitch and by the rate of change of the dynamics. Control behavior was mainly affected in the axis containing the time-varying controlled dynamics. However, control behavior in the axis not containing the time-varying dynamics was also affected, indicating cross coupling in human perception and control processes between roll and pitch. The maximum likelihood estimation method provided accurate parameter estimations when applied to a pilot model with time-dependent sigmoid functions. The parameters defining pilots' equalization dynamics after the transition in controlled dynamics and the maximum rate of change of the equalization dynamics had the lowest estimation accuracy.

Nomenclature

A_t	=	sinusoid amplitude, deg
B	=	bias
e	=	error, deg
f_t	=	target forcing function, deg
G	=	maximum rate of change, s^{-1}
H_c	=	controlled dynamics response
H_{ol}	=	pilot–vehicle open-loop response
H_p	=	pilot response
H_n	=	remnant filter
j	=	imaginary unit
K_c	=	vehicle dynamics gain
K_n	=	pilot remnant gain
K_v	=	pilot visual gain
k	=	sinusoid index
M	=	time of maximum rate of change, s
N	=	number of points
n	=	pilot remnant signal, deg
n_t	=	forcing function frequency integer factor
P_n	=	pilot remnant intensity
P_1	=	initial parameter function value
P_2	=	final parameter function value
s	=	Laplace variable
T_L	=	pilot lead time constant, s
T_m	=	measurement time, s
t	=	time, s
u	=	pilot control signal, deg
w	=	white-noise signal, deg
ζ_{nm}	=	pilot neuromuscular damping
$\boldsymbol{\Theta}$	=	parameter vector
θ	=	pitch angle, deg
τ_e	=	effective time delay, s
τ_v	=	pilot visual delay, s
ϕ	=	roll angle, deg
ϕ_t	=	sinusoid phase shift, rad
φ_m	=	phase margin, deg
ω	=	frequency, rad · s^{-1}
ω_b	=	vehicle dynamics break frequency, rad · s^{-1}
ω_c	=	crossover frequency, rad · s^{-1}
ω_{nm}	=	pilot neuromuscular frequency, rad · s^{-1}
ω_t	=	sinusoid frequency, rad · s^{-1}

Received 17 July 2015; revision received 24 October 2015; accepted for publication 31 October 2015; published online 11 January 2016.

*Senior Research Engineer, Human Systems Integration Division; peter.m.t.zaal@nasa.gov. Member AIAA.

I. Introduction

IN MANY aircraft control tasks, pilots consciously or subconsciously adapt their control behavior to controlled aircraft dynamics that change over time. These time-varying aircraft dynamics can be introduced by changing external conditions, flight mode transitions, or adaptive fly-by-wire control laws [1,2]. Past manual control studies mainly focused on operator control behavior in single-axis control tasks. A few studies focused on control behavior in multi-axis control tasks but with constant controlled dynamics [3–6]. A recent study focused on the modeling of human pilot adaptation to time-varying controlled dynamics in multi-axis control tasks; however, the parameters of the developed pilot model were not estimated from experimental data [7]. As a result, little is known about the adaptation of manual control behavior to time-varying aircraft dynamics and the interactions between multiple axes of control.

This paper presents the results of an experiment conducted to investigate how pilot control behavior in a roll–pitch control task is affected by time-varying controlled dynamics. The experiment addressed three main questions. How is manual control behavior affected when the controlled dynamics in the pilot–vehicle crossover-frequency range change from integrator to double-integrator dynamics? How does the rate at which the controlled dynamics change affect the adaptation of manual control behavior? And how do changes in the controlled dynamics of one axis affect pilot control behavior in the other axis? A genetic maximum likelihood estimation (MLE) procedure was used in conjunction with a pilot model with time-dependent sigmoid functions to characterize time-varying pilot control behavior from experimental data.

The paper is structured as follows. The roll–pitch control task, controlled dynamics, and pilot model are described first. Next, the paper provides a performance analysis of the MLE procedure used for the estimation of time-varying pilot model parameters. This is followed by a description of the experimental design and presentation of the results. The paper ends with a discussion and conclusions.

II. Roll–Pitch Control Task

A. Task Setup

Figure 1 depicts the multi-axis control task used to analyze time-varying pilot control behavior in this paper. Pilots controlled the roll and pitch attitude of an aircraft with roll dynamics $H_{c\phi}$ and pitch dynamics $H_{c\theta}$ by making control inputs u_ϕ and u_θ with a joystick. No cross coupling was present between the roll and pitch dynamics. The pilots' task was to follow the desired roll and pitch attitudes provided by the forcing functions $f_{t\phi}$ and $f_{t\theta}$ by minimizing roll and pitch errors e_ϕ and e_θ on the primary flight display (PFD) depicted in Fig. 2.

In single-loop control tasks, pilot control behavior can be modeled by a linear response function H_p and a remnant signal n that accounts for nonlinear behavior [8]. Because no cross coupling is present between the roll and pitch dynamics, the pilot–vehicle system in Fig. 1 is assumed to consist of two independent single-loop control loops. This assumption has been used in previous studies and was found appropriate for data analysis purposes [3,9]. This allows for pilot control behavior in the roll–pitch control task to be modeled by two independent linear response functions $H_{p\phi}$ and $H_{p\theta}$ and two independent remnant signals n_ϕ and n_θ.

Techniques for the identification and parameterization of the pilot response functions are well established for vehicle dynamics H_c that are constant over time [8,10,11]. However, the vehicle dynamics in Fig. 1 change over time. As a result, pilots will adapt their control behavior over time to maintain adequate levels of performance and stability margins. The goal of this study is to quantify this adaptation in pilot control behavior by estimating time-varying pilot model parameters using maximum likelihood estimation [12].

B. Time-Dependent Parameter Function

In this study, time variations in pilot control behavior were introduced by substituting constant model parameters of a conventional human operator model with time-dependent parameter functions [12]. Many types of functions can be used to describe a parameter change over time. The parameter function considered here is the sigmoid function, which is widely used for learning curve and growth modeling. This function describes the transition from an initial parameter value to a final parameter value, while allowing for control of the maximum rate of change and the time this maximum rate occurs. The sigmoid function as a function of time t is defined by

$$P(t) = P_1 + \frac{P_2 - P_1}{1 + e^{-G(t-M)}} \tag{1}$$

where P_1 is the initial parameter value, and P_2 is the final parameter value. The time of maximum rate of change is defined by M and the maximum rate of change by G. Figure 3 depicts the sigmoid function for variations of M and G. For $G \to \infty$, the function converges to a step function, describing an instant change in the parameter value.

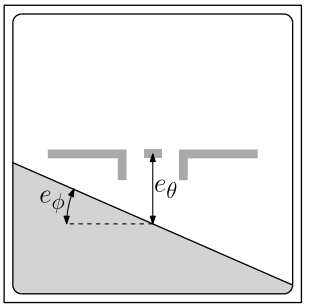

Fig. 2 Primary flight display.

Note that, for $G = 10$ s^{-1}, the function already approaches a step function in Fig. 3b.

C. Controlled Dynamics

The time-varying roll and pitch dynamics in Fig. 1 were defined by

$$H_{c\phi}(s,t) = H_{c\theta}(s,t) = \frac{K_c(t)}{s^2 + \omega_b(t)s} \tag{2}$$

where the gain $K_c(t)$ and the break frequency $\omega_b(t)$ were time-varying parameters defined by the parameter function given in Eq. (1). The initial and final parameter function values were $K_{c1} = 90.0$, $K_{c2} = 30.0$, $\omega_{b1} = 6.0$ rad $\cdot$ s^{-1}, and $\omega_{b2} = 0.2$ rad $\cdot$ s^{-1}. The time of maximum rate of change was $M = 50.0$ s, and the maximum rate of change was either $G = 0.5$ s^{-1} or $G = 100.0$ s^{-1} (see Sec. IV.A.1). These values for M and G were equivalent for both time-varying parameters of the controlled dynamics. Given the parameter functions described previously, the aircraft dynamics changed over time from $H_{c1} = 90.0/(s^2 + 6.0s)$ to $H_{c2} = 30.0/(s^2 + 0.2s)$.

Figure 4 depicts the time-varying controlled dynamics for different time instances. Note that the dynamics changed from mostly integrator dynamics ($1/s$) to mostly double-integrator dynamics ($1/s^2$) in the human crossover frequency range (1–5 rad $\cdot$ s^{-1}).

D. Pilot Model

The crossover model theorem states that human operators adapt their control behavior such that the pilot–vehicle open-loop response in the crossover region can be described by

$$H_{ol}(s) = H_p(s)H_c(s) \approx \frac{\omega_c}{s} e^{-s\tau_e} \tag{3}$$

where ω_c is the crossover frequency, and τ_e is the effective time delay [8]. Given the controlled dynamics $H_{c\phi}$ and $H_{c\theta}$, the equalization dynamics of the pilot model need to contain a lead time constant in order for Eq. (3) to hold. The pilot lead time constant was expected to

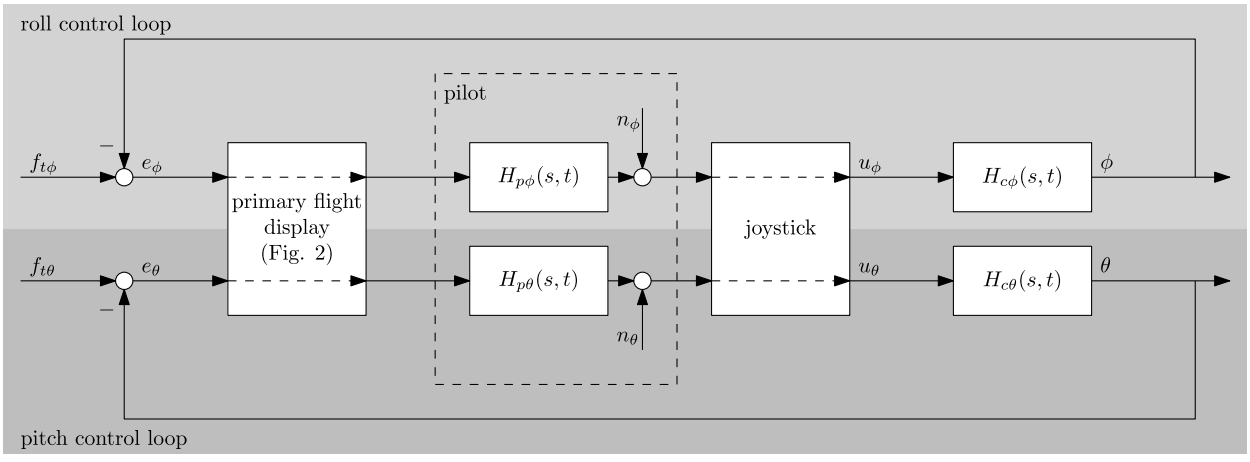

Fig. 1 Multi-axis closed-loop control task.

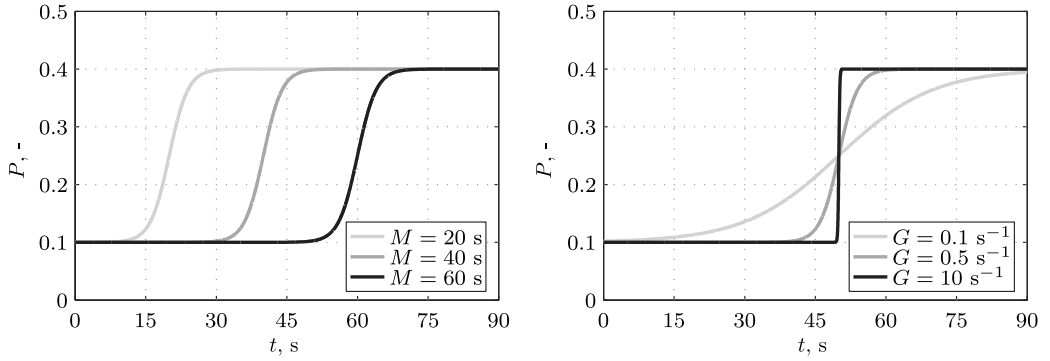

a) M variation ($P_1 = 0.1$, $P_2 = 0.4$, $G = 0.5$ s^{-1}) **b) G variation ($P_1 = 0.1$, $P_2 = 0.4$, $M = 50$ s)**

Fig. 3 Sigmoid function parameter variation.

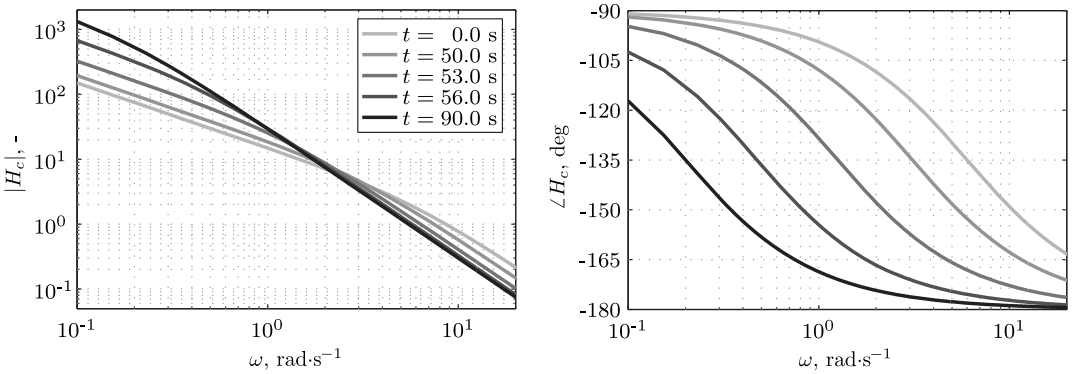

a) Controlled dynamics magnitude **b) Controlled dynamics phase**

Fig. 4 Frequency response of the aircraft dynamics at different time instances.

increase over time (lead is generated at increasingly lower frequencies) as the break frequency of the aircraft dynamics decreases. Based on previous research, the pilot gain was also expected to change over time [13,14]. The time-varying pilot model capable of modeling this adaptation in pilot control behavior is defined by

$$H_p(s,t) = \overbrace{K_v(t)[1 + T_L(t)s]}^{\text{equalization}} \overbrace{e^{-s\tau_v} \frac{\omega_{\text{nm}}^2}{\omega_{\text{nm}}^2 + 2\zeta_{\text{nm}}\omega_{\text{nm}}s + s^2}}^{\text{limitations}} \tag{4}$$

The pilot equalization dynamics consisted of a time-varying gain $K_v(t) = K_{v1} + [K_{v2} - K_{v1}]/[1 + e^{-G(t-M)}]$ and a time-varying lead time constant $T_L(t) = T_{L1} + [T_{L2} - T_{L1}]/[1 + e^{-G(t-M)}]$. The pilot limitations, defined by the time delay τ_v, neuromuscular damping ζ_{nm}, and neuromuscular frequency ω_{nm}, were assumed to be constant. Previous research found that these pilot limitation parameters are not significantly different when controlling dynamics similar to H_{c1} or H_{c2} [13,14]. The time of maximum rate of change and the maximum rate of change of both parameter functions were assumed to be equal. The resulting parameter vector $\boldsymbol{\Theta} = [K_{v1} \quad K_{v2} \quad T_{L1} \quad T_{L2} \quad M \quad G \quad \tau_v \quad \zeta_{\text{nm}} \quad \omega_{\text{nm}}]$, with a total of nine parameters, was estimated for each controlled axis.

E. Forcing Functions

Both forcing functions in Fig. 1 were sums of sines defined by the following equation:

$$f_{t\phi,t\theta}(t) = \sum_{k=1}^{N_t} A_t(k) \sin[\omega_t(k)t + \phi_{t\phi,t\theta}(k)] \tag{5}$$

where $N_t = 10$ is the number of sine waves, and ω_t, A_t, and $\phi_{t\phi,t\theta}$ are the frequency, amplitude and phase shift of the kth sine wave, respectively. The length of an experiment run was $T = 90.00$ s. The measurement time used to construct the forcing functions was $T_m = 81.92$ s. With a data sampling frequency of 100 Hz, this measurement time contains the highest power-of-two data points ($N_m = 8192$) in the total length of an experiment run. The sinusoid frequencies $\omega_t(k)$ were all integer multiples of the measurement-time base frequency $\omega_m = 2\pi/T_m = 0.0767$ rad · s^{-1} and were covering the frequency range relevant to human manual control (0.1–18 rad · s^{-1}). The spacing between the frequencies was approximately equal on a logarithmic scale.

The absolute value of a second-order low-pass filter at a sinusoid frequency was used to determine the amplitudes of the individual sine waves:

$$A_t(k) = \left| \frac{[1 + 0.1j\omega_t(k)]^2}{[1 + 0.8j\omega_t(k)]^2} \right| \tag{6}$$

The second-order low-pass filter reduced amplitudes at higher frequencies, yielding a more feasible control task. The final amplitude distributions were scaled to produce roll and pitch disturbance forcing functions with a standard deviation of 1.5 deg.

To determine the forcing function phase distributions, a large number of random phase sets were generated. The set yielding a signal with a probability distribution closest to a Gaussian distribution, without leading to excessive peaks, was selected [15]. The characteristics of the forcing functions are summarized in Table 1. Note that the roll and pitch disturbance forcing functions contained the same frequencies and amplitudes. However, the phase distributions of the two forcing functions were different. This ensured that spectral power and frequency content of the forcing functions were equivalent in both axes, while the signals appeared to be different.

III. Parameter Estimation Performance

Techniques for the identification and prediction of human operator control behavior in control tasks with constant controlled dynamics are well established and are proven to provide accurate results

Table 1 Forcing function properties

k	n_t	ω_t, rad · s^{-1}	A_t, deg	$\phi_{t\phi}$, rad	$\phi_{t\theta}$, rad
1	3	0.230	1.186	0.974	−0.753
2	5	0.384	1.121	−3.026	1.564
3	8	0.614	0.991	0.744	0.588
4	13	0.997	0.756	−2.300	−0.546
5	22	1.687	0.447	2.984	0.674
6	34	2.608	0.245	−2.513	−1.724
7	53	4.065	0.123	2.211	−1.963
8	86	6.596	0.061	1.004	−2.189
9	139	10.661	0.036	−2.255	0.875
10	229	17.564	0.025	2.210	0.604

[8,10,11,16–18]. However, insufficient techniques exist for the identification of time-varying operator control behavior and the estimation of time-varying operator model parameters. In the last decade, work on the identification of time-varying pilot control behavior focused on the use of wavelet transforms to identify time-varying pilot frequency response functions [12,19–21]. However, the wavelet transform does not allow for the estimation of time-varying pilot model parameters directly. A second step is required, fitting a pilot model frequency response to the wavelet frequency response [12,17].

To estimate time-varying pilot model parameters in the current study, a genetic MLE method commonly used for the estimation of time-invariant pilot model parameters was used [18]. The time-variation of the parameters was introduced by implementing time-dependent sigmoid functions into the pilot model (Sec. II.D), increasing the number of free parameters to be estimated. To verify that this procedure holds accurate parameter estimation results, a Monte Carlo analysis with 140 simulations was performed to determine the bias and variance characteristics of the parameter estimates. The simulations were performed using the simplified control loop depicted in Fig. 5.

The time-varying aircraft dynamics $H_{c\theta}$, pilot dynamics $H_{p\theta}$, and forcing function $f_{t\theta}$ used in the simulations are defined in Secs. II.C, II.D, and II.E, respectively. The maximum rate of change of the time-varying controlled dynamics was set to $G = 0.5$ s^{-1} and the time of the maximum rate of change to $M = 50.0$ s. The parameters of the time-varying pilot model were determined using data from a test experiment: $K_{v1} = 0.09$, $K_{v2} = 0.07$, $T_{L1} = 0.4$ s, $T_{L2} = 1.2$ s, $M = 50.0$ s, $G = 0.5$ s^{-1}, $\tau_v = 0.28$ s, $\zeta_{\text{nm}} = 0.35$, and $\omega_{\text{nm}} = 11.25$ rad · s^{-1}.

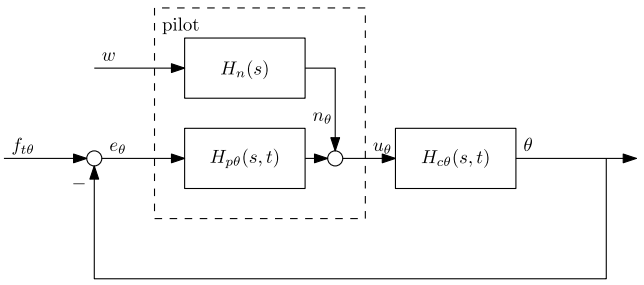

Fig. 5 Single-loop control task used for simulations.

The pilot remnant n_θ was simulated using a low-pass-filtered white-noise signal w. The remnant filter was defined by $H_n = K_n/(0.2s + 1)$. Three levels of pilot remnant intensity $P_n = \sigma^2(n)/\sigma^2(u)$ were used to investigate the effect of remnant intensity on the bias and variance of the parameter estimates. The filter gain K_n was selected to induce remnant intensities of $P_n = 0.05$, $P_n = 0.15$, and $P_n = 0.25$.

Figures 6a and 6b depict the relative bias and variance, respectively, of the pilot model parameters for different levels of remnant intensity. The relative bias and variance are calculated by dividing the bias and variance of each parameter by the real parameter value. Figure 6a indicates that the bias increases for most of the parameters as the remnant intensity increases. Furthermore, the bias of K_{v2}, T_{L2}, and G is higher compared to the other variables. Figure 6b shows that the relative variance of the parameters also increases as the remnant intensity increases, an expected result. The figure further indicates that the variance of the final parameter function values K_{v2} and T_{L2} is higher compared to the initial values K_{v1} and T_{L1}. Finally, it can be observed that the maximum rate of change G has the highest variance of all parameters.

These results indicate that the final parameter function variables K_{v2} and T_{L2} as well as the maximum rate of change G will most likely have the lowest accuracy when estimated from experiment data. However, note that the presented results are for this particular set of pilot model parameters. The true pilot model parameter bias and variance characteristics will depend on a number of factors, such as performance, remnant characteristics, and control behavior of individual pilots.

IV. Experiment Setup

A. Method

1. *Independent Variables*

Two independent variables were used in the experiment: 1) the axis of the time-varying aircraft dynamics (roll, pitch, or both axes), and 2) the maximum rate of change of the time-varying aircraft dynamics ($G = 0.5$ s^{-1} or $G = 100.0$ s^{-1}). A full-factorial design was implemented, resulting in six conditions. Two additional conditions with constant H_{c1} or H_{c2} dynamics were performed as reference conditions, resulting in eight conditions in total (Table 2).

Conditions 1 and 2, referred to by the symbols C1 and C2, had constant dynamics (H_{c1} or H_{c2}) in both the roll and pitch axes. Conditions 3 to 5 (C3–C5) had time-varying dynamics ($H_{c1} \rightarrow H_{c2}$) with a maximum rate of change of 0.5 s^{-1} in one or both of the axes. This maximum rate of change resulted in a gradual change from H_{c1} to H_{c2} in about 20 s. In conditions 6 to 8 (C6–C8), the axes containing the time-varying dynamics were equivalent to C3–C5. However, the time-varying dynamics had a maximum rate of change of 100.0 s^{-1},

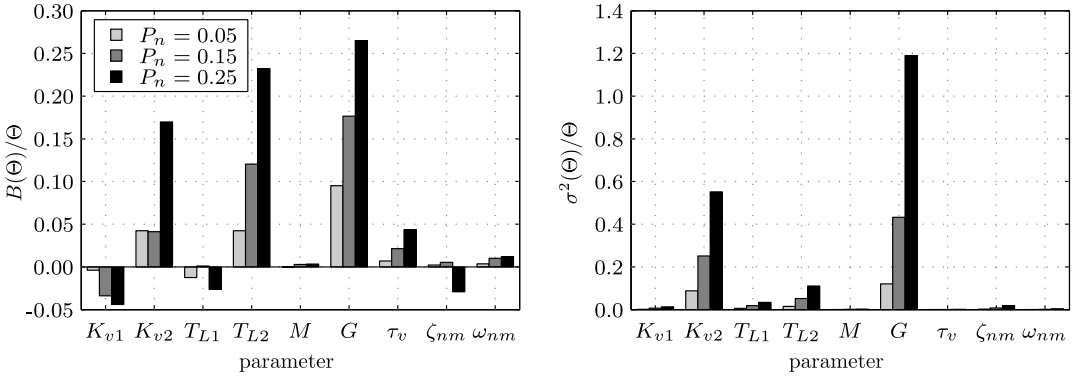

a) Pilot model parameter bias **b) Pilot model parameter variance**

Fig. 6 Relative bias and variance of the time-varying pilot model parameters (140 simulations).

Table 2 Experiment conditions

Condition	Roll dynamics	Pitch dynamics	Maximum rate of change	
C1	H_{c1}	H_{c1}		
C2	H_{c2}	H_{c2}		
C3	$H_{c1} \rightarrow H_{c2}$	H_{c1}	0.5 s^{-1}	
C4	H_{c1}	$H_{c1} \rightarrow H_{c2}$	0.5 s^{-1}	
C5	$H_{c1} \rightarrow H_{c2}$	$H_{c1} \rightarrow H_{c2}$	0.5 s^{-1}	
C6	$H_{c1} \rightarrow H_{c2}$	H_{c1}	100.0 s^{-1}	
C7	H_{c1}	$H_{c1} \rightarrow H_{c2}$	100.0 s^{-1}	
C8	$H_{c1} \rightarrow H_{c2}$	$H_{c1} \rightarrow H_{c2}$	100.0 s^{-1}	

resulting in an almost instant (steplike) change from H_{c1} to H_{c2}. The aircraft dynamics H_{c1} and H_{c2} are defined in Sec. II.C.

2. Apparatus

Figure 2 shows the PFD used to provide pilots with roll and pitch error information. The PFD was depicted on a ViewSonic G225f CRT monitor. This monitor has a viewing area with a diagonal of 20 in. and was set to a display resolution of 1600×1200 pixels. The PFD was depicted in the center of the screen and had a size of 400×400 pixels. The thickness of the aircraft symbol was 6 pixels, and the thickness of the horizon was 2 pixels. The roll angle was magnified by a factor of 2 on the display. One degree of pitch angle was visible by an 8 pixel translation of the horizon from the center of the aircraft symbol (see Fig. 2). Pilots were seated at a distance of approximately 1.8 ft from the monitor.

A Logitech Extreme 3D Pro joystick was used to make control inputs. This right-handed joystick has considerable breakout force. Joystick output values in the roll and pitch axes ranged from -1.0 to 1.0, corresponding to full left–right and fore–aft joystick deflections, respectively.

3. Participants and Instructions

Nine general aviation pilots participated in the experiment. All were male with an average age of 24.3 years. The average total of flying hours was 773.2 h with an average of 78.2 flying hours in the last six months. All pilots were right-handed, and only one had previous experience with the type of control task used.

Every pilot received a briefing before the start of the experiment. The briefing contained information about the objective of the study. In addition, pilots were given details about the control task, conditions, and procedures of the experiment. Pilots were instructed to make control inputs in an active and continuous manner, trying to minimize the roll and pitch errors presented on the visual display to the best of their capabilities. In addition, they were told to focus on minimizing roll and pitch errors at the same time.

4. Procedures

All experimental runs had a length of 90.0 s. The first 8.08 s of a run were considered the run-in time. During this phase, pilots were able to stabilize the controlled dynamics and adjust to the task. Data from the last 81.92 s were used as measurement data for data analysis (see Sec. II.E).

All pilots performed a total of 96 runs. The experiment consisted of four segments, each containing 24 runs. Each of the eight conditions was presented three times in every segment. The conditions were presented in a quasi-random order using a Latin-square design. Pilots were not informed about which condition they were performing.

The first two segments were used for training, and runs from the last two segments were used for the final data analysis. After every run, tracking performance, defined as the root mean square (RMS) of the roll and pitch errors, was presented to the pilots to motivate them to constantly perform at their maximum level of performance. In between each segment, the experimenter made sure pilots reached and maintained asymptotic performance for each condition, that is, more or less constant RMS values.

In each segment, pilots were able to go through the experiment at their own pace. They were able to start the next run by pressing the trigger on the joystick. This allowed them to take breaks at any time. Every pilot was able to complete the experiment within 4 h.

5. Dependent Measures

Several dependent measures were calculated from the experiment data. First, pilot performance and control activity in the roll and pitch axes were evaluated in terms of the RMS of the error and control signals, respectively. Next, the parameters of the time-varying pilot model were estimated using the MLE method discussed in [18]. For every participant and condition, the parameter estimation was performed on experimental data averaged over six runs. The control signal variance accounted for (VAF) was calculated as a measure for pilot model accuracy in explaining the measured control signal data. Finally, time-varying pilot–vehicle open-loop responses as well as corresponding time-varying crossover frequencies and phase margins were calculated to determine the performance and stability margins of the combined pilot–vehicle system.

B. Hypotheses

In conditions in which the aircraft dynamics change from H_{c1} to H_{c2}, we hypothesized that pilot roll and pitch target-following performance decreases, and roll and pitch control activity increases over time [13,14]. Furthermore, crossover frequencies increase and phase margins decrease. Finally, the pilot visual gain K_v and visual lead time constant T_l were expected to decrease and increase, respectively, when the dynamics change from H_{c1} to H_{c2} [13]. We expected overall tracking performance to degrade when the controlled dynamics in the two axes are different, that is, if the controlled dynamics change in one axis only [3,4].

The remnant intensity levels in a multi-axis control task were expected to be higher than in a single-axis control task, due to the fact that attention must be split. Because the analysis in Sec. III found that the bias and variance of the parameters specifying the final parameter-function values and the maximum rate of change were higher compared to other parameters, we expected a relatively large uncertainty in estimations of K_{v2}, T_{l2}, and G. In addition, we hypothesized that the accuracy of the overall pilot model (as determined by the VAF) would be higher for controlled dynamics H_{c2} [22].

V. Results

This section provides the combined results of the nine pilots that participated in the experiment. The error bars in the error-bar plots are corrected for between-subject variability by normalizing the subject means across conditions [23]. The data from the reference conditions C1 and C2 are marked by gray continuous and dashed lines, respectively. A paired-samples T-test was performed on the dependent measures from the two reference conditions to reveal statistically significant differences between them. A repeated-measures analysis of variance was used to detect statistically significant differences between the conditions with time-varying aircraft dynamics.

A. Pilot Performance and Control Activity

Pilot performance and control activity in the roll axis, defined by the RMS of the roll error and the RMS of the roll control signal, are depicted in Figs. 7a and 7b, respectively. Figures 8a and 8b provide the same data for the pitch axis. A lower roll or pitch error RMS indicates a higher performance, and a lower control signal RMS indicates a lower control activity. Note that these measures were calculated over the entire run and thus, for the conditions with time-

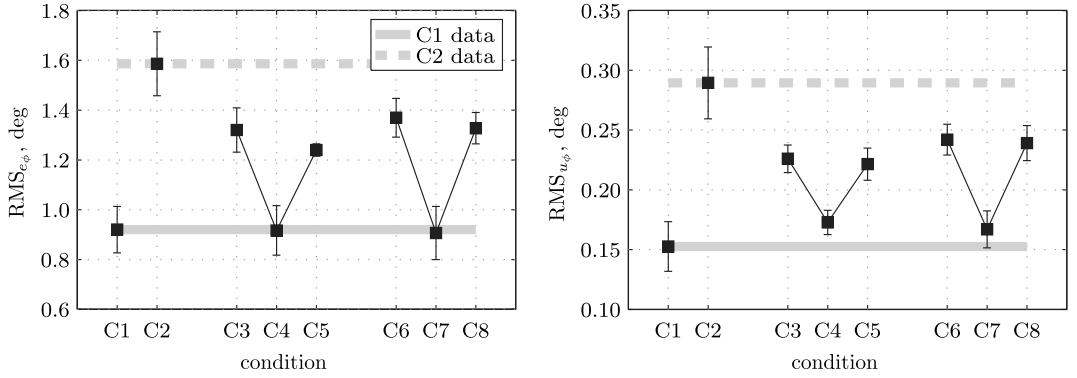

a) Roll error signal **b) Roll control signal**

Fig. 7 Roll tracking performance and control activity.

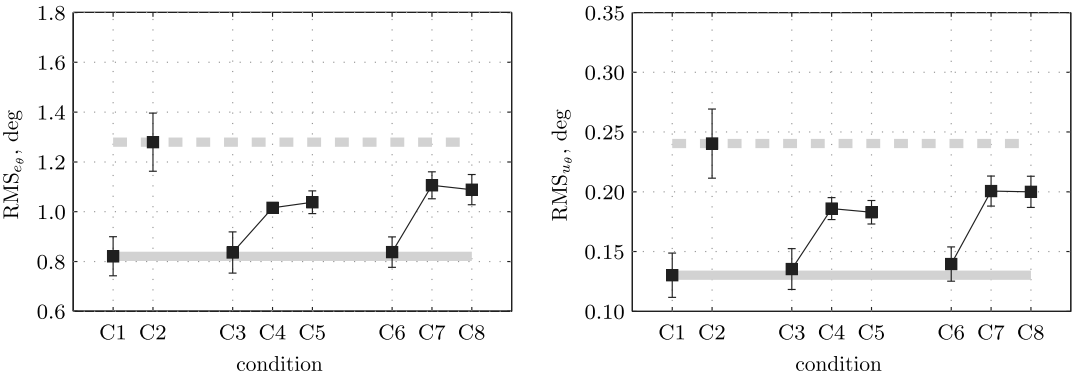

a) Pitch error signal **b) Pitch control signal**

Fig. 8 Pitch tracking performance and control activity.

varying dynamics, include performance and control activity during the control of steady H_{c1} and H_{c2} dynamics and the transition phase.

Figure 7a indicates that performance in the roll axis was higher for the reference condition C1 with H_{c1} controlled dynamics compared to reference condition C2 with H_{c2} dynamics, a statistically significant difference, $t(8) = 7.047$, $p < 0.001$. This result has also been observed in single-axis control studies [13]. In the conditions with time-varying dynamics, a statistically significant interaction was found between the axis of the dynamics change and the maximum rate of change, $F(2, 16) = 5.500$, $p = 0.015$. No statistically significant difference in performance between the two maximum rates of change was found for the conditions with a change in roll dynamics only (C3 and C6), $F(1, 8) = 3.527$, $p = 0.097$. Also, for the conditions with a change in pitch dynamics only (C4 and C7), no significant difference between the two maximum rates of change was found, $F(1, 8) = 0.712$, $p = 0.423$. However, for the conditions with a change in both roll and pitch dynamics, performance was statistically significantly lower (higher RMS$_{e\phi}$) for the higher maximum rate of change, $F(1, 8) = 14.170$, $p = 0.006$. Performance in the conditions with changing roll dynamics was in between the performance for C1 and C2. Performance in the conditions with a change in pitch dynamics only was equal to the performance in C1.

Figure 7b indicates that control activity was significantly higher for condition C2 compared to C1, $t(8) = 6.271$, $p < 0.001$. A statistically significant difference in roll control activity was introduced by the axis of the dynamics change for conditions with a change in controlled dynamics, $F(2, 16) = 55.227$, $p < 0.001$. Post hoc analysis with a Bonferroni adjustment revealed that the significant differences in roll control activity were between conditions with a change in roll dynamics only and a change in pitch dynamics only, $p < 0.001$, and second, between a change in pitch dynamics only and a change in both roll and pitch dynamics, $p < 0.001$. There was no statistically significant difference between conditions with a change in roll dynamics only and a change in both roll and pitch dynamics, $p = 1.000$. No significant difference was introduced by the maximum rate of change, $F(2, 16) = 4.419$, $p = 0.069$.

The performance changes in the pitch axis when the pitch controlled dynamics in the pilot–vehicle crossover-frequency range change from H_{c1} to H_{c2} dynamics were very similar to the roll performance changes when the roll controlled dynamics change. Figure 8a indicates that disturbance-rejection performance was significantly better in the condition with constant H_{c1} dynamics C1 compared to the condition with constant H_{c2} dynamics C2, $t(8) = 5.457$, $p = 0.001$. For conditions C3–C8, a statistically significant difference in pitch performance was introduced by the axis of the changing dynamics, $F(2, 16) = 26.606$, $p < 0.001$, and the maximum rate of change of the dynamics, $F(2, 16) = 6.406$, $p = 0.035$. Post hoc analysis with Bonferroni adjustment revealed that performance in the conditions with a change in roll dynamics only was statistically significantly higher compared to performance in the conditions with a change in pitch dynamics only, $p = 0.002$, and conditions with a change in both roll and pitch dynamics, $p = 0.003$. Performance between the conditions with a change in pitch dynamics was not significantly different, $p = 1.000$. Performance was lower in the conditions with the higher maximum rate of change, $p = 0.035$.

Figure 8b indicates that pitch control activity was significantly higher for the condition with constant H_{c2} dynamics compared to the condition with constant H_{c1} dynamics, $t(8) = 5.466$, $p = 0.001$. Pitch control activity was statistically significantly affected by the axis of the time-varying dynamics, $F(2, 16) = 28.179$, $p < 0.001$, and the maximum rate of change, $F(2, 16) = 17.670$, $p = 0.003$. Following the same trend as the pitch performance, the pitch control activity in both the conditions with a dynamics change in pitch only and the conditions with a dynamics change in roll and -pitch was significantly higher than in the conditions with a roll dynamics change only, $p = 0.001$ and $p = 0.003$, respectively. Control activity between the conditions with a change in pitch dynamics was not significantly different, $p = 1.000$. Pitch control

activity was statistically significantly higher in the conditions with a higher maximum rate of change (C6–C8).

Finally, by comparing performance and control activity between the roll and pitch axes (comparing Figs. 7 and 8), it can be observed that the performance in reducing the disturbance was higher, and control activity was lower in the pitch axis, both significant differences, $F(1,8) = 22.218$, $p = 0.002$ and $F(1,8) = 50.480$, $p < 0.001$, respectively.

B. Pilot Model Variance Accounted For

For conditions with time-varying controlled dynamics (C3–C8), the parameters of the pilot model $H_p(s,t)$ discussed in Sec. II.D were estimated from experiment data using a genetic MLE method. For the conditions with constant controlled dynamics (C1 and C2), a pilot model $H_p(s)$ was used without time-dependent sigmoid functions, reducing the number of parameters to five with $\boldsymbol{\Theta} = [K_{v1} \quad T_{L1} \quad \tau_v \quad \zeta_{\text{nm}} \quad \omega_{\text{nm}}]$.

Figures 9 and 10 depict the pilot model VAF for the roll and pitch control signals, respectively. A higher VAF indicates that a larger percentage of the measured control signal variance can be explained by the pilot model. For conditions C3–C8, in addition to the model with time-dependent sigmoid functions, the VAF was also calculated for the pilot model with constant parameters, as used for C1 and C2. This allows us to determine if a pilot model with time-dependent sigmoid functions was indeed more suitable to describe the measured data in the conditions with time-varying controlled dynamics than a model with constant parameters.

Figure 9 reveals, as hypothesized in Sec. IV.B, that the VAF in the roll axis was significantly higher for the condition with H_{c2} dynamics C2 compared to the condition with H_{c1} dynamics C1, $t(8) = 5.059$, $p = 0.001$. For the conditions with time-varying dynamics, a statistically significant interaction was found for the VAF between the axis of the dynamics change and the type of model used, $F(2,16) = 14.616$, $p < 0.001$. In the conditions with a change in roll dynamics only (C3 and C6) and the conditions with a change in both roll and pitch dynamics (C5 and C8), the VAF for the time-varying model was statistically significantly higher than the VAF for the constant model, $F(1,8) = 55.321$, $p < 0.001$ and $F(1,8) = 40.509$, $p < 0.001$. For the conditions with a change in pitch dynamics only (C4 and C7), a less significant difference was found between the two models, $F(1,8) = 7.125$, $p = 0.028$. No significant effect from the maximum rate of change was found, $F(1,8) = 0.383$, $p = 0.553$. These results indicate that the pilot model with time-varying parameters was more suitable to describe the roll control data in the conditions with time-varying aircraft dynamics, especially in the conditions with time-varying roll dynamics.

The results in the pitch axis (Fig. 10) are very similar compared to the roll axis. The VAF in C2 was significantly higher compared to C1, $t(8) = 4.281$, $p = 0.003$. For the conditions with time-varying dynamics, two interactions were found, one between the type of model and the axis of the varying dynamics, $F(2,16) = 42.846$, $p < 0.001$, and the other between the rate of the dynamics change and the axis of the varying dynamics, $F(2,16) = 4.412$, $p = 0.030$. Comparing conditions C3 and C6 revealed a statistically significant difference introduced by the type of model, $F(1,8) = 27.556$, $p = 0.001$, and the maximum rate of change, $F(1,8) = 8.328$, $p = 0.020$. The VAF was slightly higher for the time-varying pilot model and slightly lower for the higher maximum rate of change. For the conditions with a change in pitch dynamics only (C4 and C7) as well as the conditions with a change in both roll and pitch dynamics (C5 and C8), the VAF of the time-varying pilot model was statistically significantly higher, $F(1,8) = 68.125$, $p < 0.001$ and $F(1,8) = 86.280$, $p < 0.001$, respectively. This indicates that the model with time-varying parameter functions was more suitable to describe the pitch control data in the conditions with time-varying aircraft dynamics, especially in the conditions with time-varying pitch dynamics.

Comparing the VAF between the roll and pitch axes (Fig. 9 compared to Fig. 10) revealed that the VAF in the pitch axis was significantly higher, $F(1,8) = 107.690$, $p < 0.001$. This might indicate that pilots behaved more linearly (i.e., introduced less remnant) in the pitch axis because a higher percentage of the data could be explained by the linear pilot model.

C. Pilot Model Parameters

Figures 11 and 12 present the estimated parameters for the pilot model in roll and pitch, respectively. Black squares depict the model parameters that are present in both the constant and time-varying pilot models. White squares depict model parameters that are available in the time-varying pilot model only.

Results from the paired-samples T-test indicated that, for the roll axis, there was no significant difference in the visual gain K_{v1} between the condition with constant H_{c1} dynamics C1 and the condition with constant H_{c2} dynamics C2, $t(8) = 1.469$, $p = 0.180$ (Fig. 11a). However, the data suggested that K_{v1} was slightly lower in condition C2. For the conditions with time-varying dynamics, a statistically significant difference between the initial and final parameter value, $F(1,8) = 8.604$, $p = 0.019$, and the axis of the changing dynamics was found, $F(1,8) = 10.536$, $p = 0.001$. No significant effect of the maximum rate of change was detected, $F(1,8) = 1.504$, $p = 0.255$. Post hoc analysis with Bonferroni adjustment revealed that the final visual gain is significantly lower than the initial gain, $p = 0.019$. The visual gain was significantly different between the conditions with a change in pitch dynamics only and a change in both roll and pitch dynamics, $p < 0.001$, but not between the other two condition pairs, $p = 0.351$ and $p = 0.130$.

The visual gain for the pilot model in pitch is given in Fig. 12a. The visual gain K_{v1} was significantly lower in C2 compared to C1, $t(8) = 5.339$, $p = 0.001$. Similar to the roll axis, a statistically significant difference between the initial and final parameter value and the axis of the changing dynamics was found for the conditions with time-varying dynamics, $F(1,8) = 69.017$, $p < 0.001$ and $F(1,8) = 4.299$, $p = 0.032$, respectively. No significant effect of the maximum rate of change was found, $F(1,8) = 0.412$, $p = 0.539$. Post hoc analysis revealed that the final visual gain is significantly lower than the initial gain, $p < 0.001$. Furthermore, the visual gain was not significantly different between the conditions with a change in roll dynamics only and pitch dynamics only or the

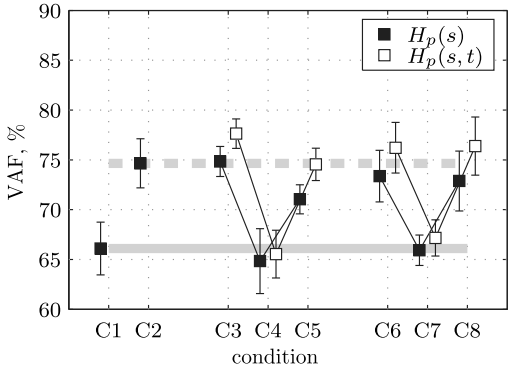

Fig. 9 Roll-axis variance accounted for.

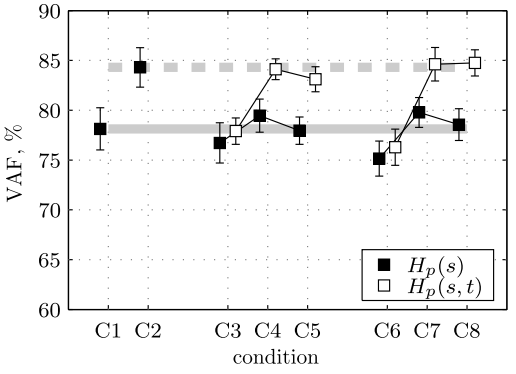

Fig. 10 Pitch-axis variance accounted for.

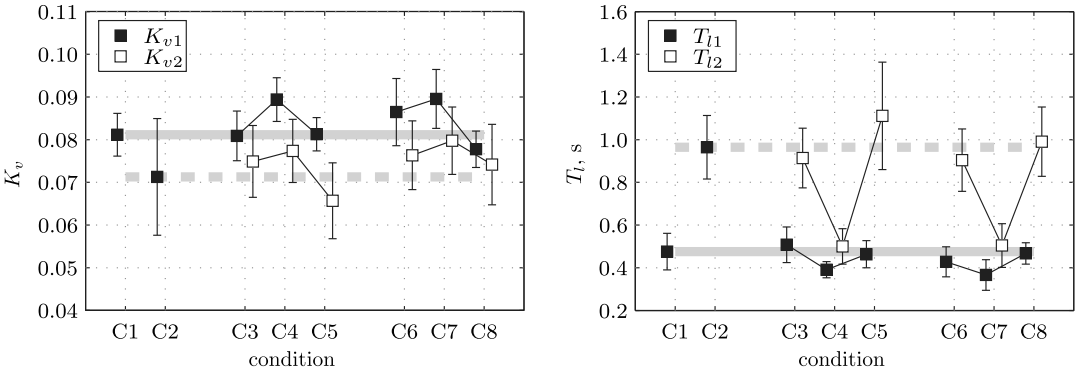

a) Roll visual gain

b) Roll lead time constant

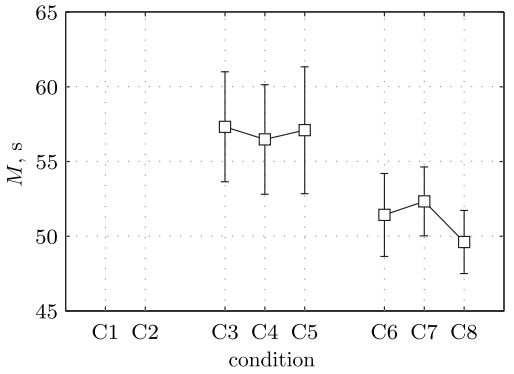

c) Roll time of maximum rate of change

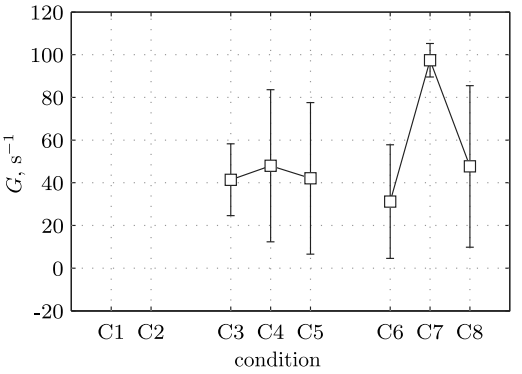

d) Roll maximum rate of change

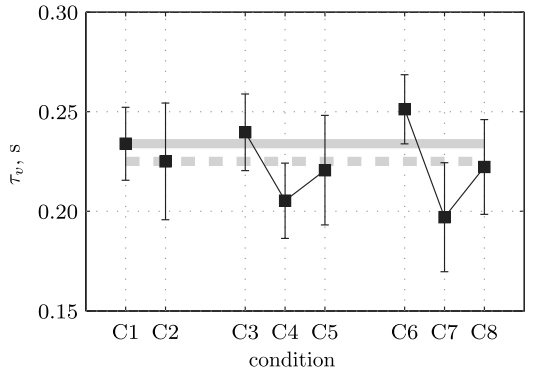

e) Roll visual delay

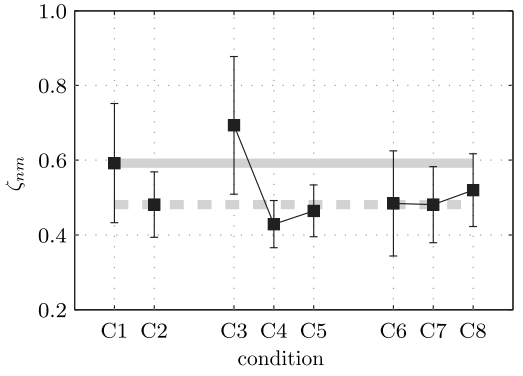

f) Roll neuromuscular damping

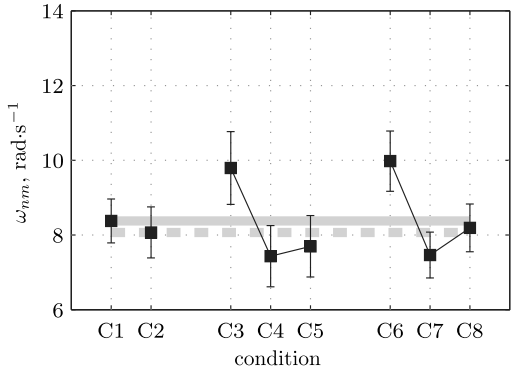

g) Roll neuromuscular frequency

Fig. 11 Means and 95% confidence intervals of the roll pilot model parameters.

conditions with a change in roll dynamics only and a change in both roll and pitch dynamics, $p = 1.000$ and $p = 0.076$. The visual gain was marginally significantly different between the conditions with a change in pitch dynamics only and a change in both roll and pitch dynamics, $p = 0.057$.

Comparing the visual gains between the roll and pitch axes (Fig. 11a with Fig. 12a), it was found that the initial visual gain K_{v1} was significantly higher in the pitch axis, $F(1, 8) = 7.469$, $p = 0.026$. The final visual gain K_{v2} was not significantly different between the roll and pitch axes, $F(1, 8) = 0.514$, $p = 0.494$.

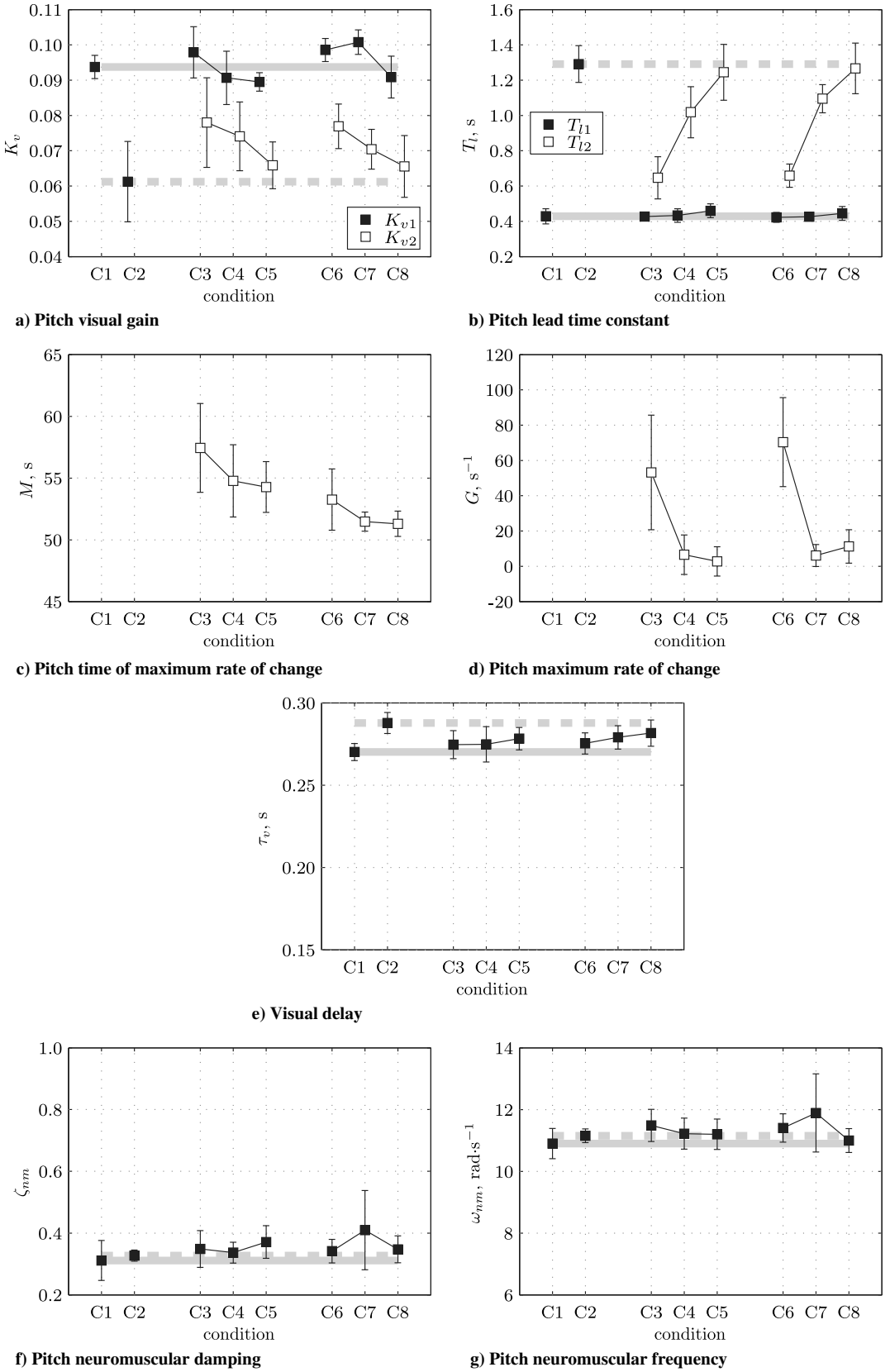

a) Pitch visual gain **b) Pitch lead time constant**

c) Pitch time of maximum rate of change **d) Pitch maximum rate of change**

e) Visual delay

f) Pitch neuromuscular damping **g) Pitch neuromuscular frequency**

Fig. 12 Means and 95% confidence intervals of the pitch pilot model parameters.

From Fig. 11b it can be observed that, in the roll axis, the visual lead T_{L1} was significantly higher in C2 compared to C1, $t(8) = 6.962$, $p < 0.001$. Based on the characteristics of the controlled dynamics, this was an expected result and supports findings from previous studies. For the conditions with time-varying dynamics, a statistically significant interaction was found between the initial and final lead time constants and the axis of the change in dynamics, $F(2, 16) = 33.628$, $p < 0.001$. For the conditions with a change in roll dynamics only and a change in both roll and pitch dynamics, the final lead time constant was significantly higher than the initial lead time constant, $F(1, 8) = 292.971$, $p < 0.001$ and $F(1, 8) = 109.967$, $p < 0.001$. For the conditions with a change in pitch dynamics only,

the final lead time constant was also statistically significantly higher, $F(1,8) = 18.900$, $p = 0.002$, but this difference was less significant than in the other conditions. No significant differences were introduced by the maximum rate of change, $F(1,8) = 0.902$, $p = 0.370$.

The effects for the visual lead time constant in the pitch axis were similar to the effects in the roll axis (Fig. 12b). In the pitch axis, the lead time constant T_{L1} was also significantly higher for condition C2 compared to C1, $t(8) = 13.806$, $p < 0.001$. As in the roll axis, in the conditions with time-varying dynamics, a statistically significant interaction was found between the initial and final lead time constants and the axis of the change in dynamics, $F(2,16) = 44.076$, $p < 0.001$. For the conditions with a change in roll dynamics only, the final lead time constant was statistically significantly higher than the initial value, $F(1,8) = 39.635$, $p < 0.001$, indicating a cross coupling between the roll and pitch axes. For the conditions with a change in pitch dynamics only and a change in both roll and pitch dynamics, the final lead time constant was also significantly higher than the initial lead time constant, $F(1,8) = 439.147$, $p < 0.001$ and $F(1,8) = 135.430$, $p < 0.001$. No significant differences were introduced by the maximum rate of change, $F(1,8) = 0.367$, $p = 0.562$.

Comparing the lead time constants between the roll and pitch axes (Fig. 11b with Fig. 12b) revealed that the initial lead time constant T_{L1} was not significantly different between the two axes, $F(1,8) = 0.884$, $p = 0.375$. The final lead time constant T_{L2} was significantly higher in the pitch axis compared to the roll axis, $F(1,8) = 8.720$, $p = 0.018$.

Figures 11c, and 12c depict the time of maximum rate of change for the roll and pitch axes, respectively. In both axes, no significant differences were introduced by the axis of the roll or pitch dynamics change, $F(1,8) = 0.283$, $p = 0.757$ and $F(1,8) = 2.507$, $p = 0.113$, respectively. However, in both axes, the maximum rate of change introduced a significant effect, $F(1,8) = 16.573$, $p = 0.004$ and $F(1,8) = 15.529$, $p = 0.004$. For the higher maximum rate of change, representing the steplike change, the time of maximum rate of change was lower, indicating that the change in pilot control behavior occurred sooner after the change in controlled dynamics at $t = 50.0$ s. No significant differences in M were found between the roll and pitch axes, $F(1,8) = 0.099$, $p = 0.762$.

The maximum rate of change G of the pilot visual gain and lead time constant is presented in Fig. 11d for the roll axis and Fig. 12d for the pitch axis. The value of the maximum rate of change had an upper bound of 100.0 s^{-1} in the estimation procedure. In the roll axis, a statistically significant interaction between the axis of the dynamics change and the maximum rate of change was found, $F(2,16) = 6.011$, $p = 0.011$. This interaction is introduced by the fact that the maximum rate of change did not introduce a statistically significant difference between conditions C3 and C6, $F(1,8) = 0.729$, $p = 0.418$, or between conditions C5 and C8, $F(1,8) = 0.057$, $p = 0.817$. However, a statistically significant difference was introduced between conditions C4 and C7, $F(1,8) = 9.558$, $p = 0.015$. Note that, above $G = 10$ s^{-1}, the time-dependent sigmoid function is basically a step function (Sec. II.B). Hence, pilot roll control behavior in the roll axis changed almost instantaneously due to a change in controlled dynamics in all conditions.

In the pitch axis, the maximum rate of change of the controlled dynamics did not affect the maximum rate of change of the change in pilot dynamics, $F(1,8) = 1.344$, $p = 0.280$. However, the maximum rate of change was significantly affected by the axis of the dynamics change, $F(2,16) = 60.643$, $p < 0.001$. Post hoc analysis with Bonferroni adjustment revealed that there was no significant difference between the conditions with a change in pitch dynamics only and the conditions with a change in both roll and pitch dynamics, $p = 1.000$. However, there was a statistically significant difference between the conditions with a change in roll dynamics only and the conditions with a change in pitch dynamics only, $p < 0.001$, and the conditions with a change in roll dynamics only and the conditions with a change in both roll and pitch dynamics, $p = 0.001$. Pilot pitch control behavior changed almost instantaneously in the conditions with a change in roll dynamics only but changed more gradually in the conditions with a change in pitch dynamics.

Comparing the values for the maximum rate of change between both axes (Fig. 11d with Fig. 12d) revealed that the maximum rate of change in the pitch axis was significantly lower, $F(1,8) = 36.409$, $p < 0.001$. Note that the error bars for the maximum rate of change are relatively large, indicating substantial variations between subjects. This is most likely caused by the lower estimation accuracy for this parameter, as found in the bias and variance analysis of Sec. III.

The pilot visual time delay τ_v is depicted in Figs. 11e and 12e for the roll and pitch axes, respectively. In the roll axis, the visual time delay was not significantly different between the two conditions with constant dynamics (C1 and C2), $t(8) = 0.509$, $p = 0.625$. This supports the assumption that this parameter does not change over time when the controlled dynamics change from H_{c1} to H_{c2}, as described in Sec. II.D. In the pitch axis, the visual time delay was significantly different between conditions C1 and C2, $t(8) = 4.353$, $p = 0.002$. However, note that the difference was only 20 ms. In the roll axis, the visual time delay was statistically significantly affected by the axis of the dynamics change, $F(1,8) = 7.817$, $p = 0.004$. Post hoc analysis with Bonferroni adjustment showed that the significant difference was between conditions with a change in roll dynamics only and the conditions with a change in pitch dynamics only, $p = 0.005$. There was no statistically significant difference between the conditions with a change in roll dynamics only and the conditions with a change in both the roll and pitch dynamics, $p = 0.086$, or between the conditions with a change in pitch dynamics only and the conditions with a change in both roll and pitch dynamics, $p = 0.590$. No significant differences were found in the roll axis from the maximum rate of change, $F(1,8) = 0.062$, $p = 0.810$. In the pitch axis, no significant differences were introduced by the axis of the dynamics change, $F(2,16) = 0.595$, $p = 0.563$, or the maximum rate of change, $F(1,8) = 4.805$, $p = 0.060$. Comparing the time delay between the roll and pitch axes (Fig. 11e with Fig. 12e) reveals that the time delay in the pitch axis was significantly higher, $F(1,8) = 19.753$, $p < 0.002$.

Figures 11f and 12f depict the neuromuscular damping for the roll and pitch axes, respectively. In both axes, the damping was not statistically significantly different between conditions C1 and C2, supporting the assumption to define this parameter as a constant parameter in $H_p(s,t)$, $t(8) = 1.361$, $p = 0.211$ and $t(8) = 0.479$, $p = 0.645$. In the roll axis, the axis of the dynamics change introduced statistically significant differences in the conditions with changing aircraft dynamics, $F(2,16) = 4.155$, $p = 0.035$. However, these differences were not detected in the post hoc analysis between any of the condition pairs, $p > 0.050$. No significant differences were introduced by the maximum rate of change of the controlled dynamics, $F(1,8) = 0.757$, $p = 0.410$. In the pitch axis, no statistically significant differences were introduced by the axis of the dynamics change, $F(1,8) = 0.348$, $p = 0.711$, or the maximum rate of change, $F(1,8) = 1.060$, $p = 0.333$. Comparing the neuromuscular damping between the two axes, the damping was found to be significantly lower in the pitch axis, $F(1,8) = 16.467$, $p = 0.004$.

The neuromuscular frequency is given in Figs. 11g and 12g for the roll and pitch axes, respectively. There was no significant difference between conditions C1 and C2 in the roll or pitch axes, supporting the assumption of this parameter being a constant parameter in the time-varying pilot model, $t(8) = 0.840$, $p = 0.425$ and $t(8) = 0.988$, $p = 0.352$. In the roll axis, a statistically significant difference was introduced by the axis of the dynamics change, $F(1,8) = 21.925$, $p < 0.001$. Post hoc analysis with Bonferroni adjustment revealed that the neuromuscular frequency in the conditions with a change in roll dynamics only was significantly higher than the frequency in the conditions with a change in pitch dynamics only, $p < 0.001$, and the conditions with a change in both roll and pitch dynamics, $p = 0.003$. No significant difference was detected between the conditions with a change in pitch dynamics only and the conditions with a change in both roll and pitch dynamics, $p = 0.887$ No significant differences were introduced by the maximum rate of change, $F(1,8) = 1.313$, $p = 0.285$. In the pitch axis, no statistically significant differences were introduced by the axis of the dynamics change, $F(1,8) = 0.870$, $p = 0.438$, or the maximum rate of change,

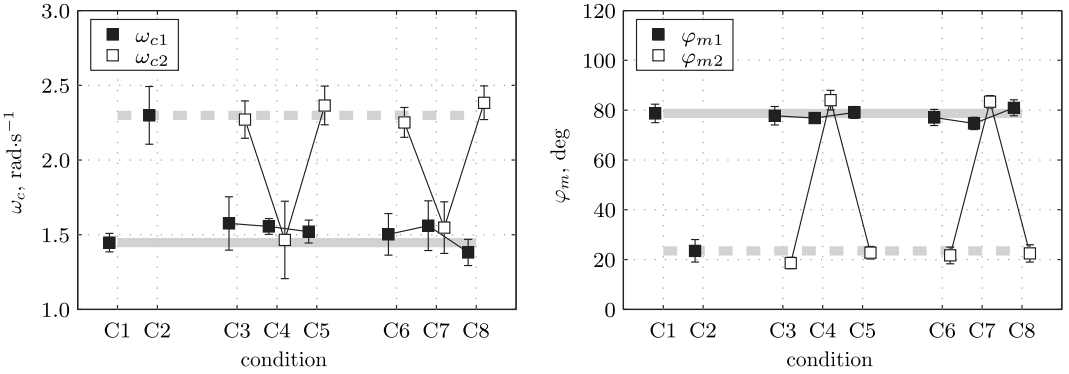

a) Roll crossover frequency **b) Roll phase margin**

Fig. 13 Roll-axis crossover frequencies and phase margins.

$F(1, 8) = 0.641$, $p = 0.446$. The neuromuscular frequency was statistically significantly higher in the pitch axis compared to the roll axis, $F(1, 8) = 44.461$, $p < 0.001$.

D. Pilot–Vehicle Open Loop

The calculated steady-state crossover frequencies and phase margins for each condition are depicted in Figs. 13 and 14 for roll and pitch, respectively. These results are presented similarly to the pilot model parameters K_v and T_l. The subscript 1 indicates the value of the crossover frequency or phase margin before the change in aircraft dynamics, whereas the subscript 2 indicates the value after the change.

Figure 13a indicates that the roll crossover frequency was higher in the condition with constant double-integrator-like dynamics C2 compared to the condition with constant single-integrator-like dynamics C1, a statistically significant effect, $t(8) = 10.458$, $p < 0.001$. For the conditions with time-varying dynamics, there was a statistically significant interaction between the axis of the dynamics change and the initial and final crossover frequencies, $F(2, 16) = 64.530$, $p < 0.001$. There was a statistically significant difference between the initial and final crossover frequency for a change in roll dynamics only (C3 and C6), $F(1, 8) = 57.542$, $p < 0.001$; no significant difference for a change in pitch dynamics only (C4 and C7), $F(1, 8) = 0.155$, $p = 0.704$; and a significant difference when both the roll and pitch dynamics changed (C5 and C8), $F(1, 8) = 78.950$, $p < 0.001$. In the conditions with changing roll dynamics, the final roll crossover frequency was equal to the crossover frequency in C2. In the conditions with a change in pitch dynamics only, the crossover frequency remained constant ($\omega_{c1} = \omega_{c2}$) and was equal to the crossover frequency in C1. The maximum rate of change did not introduce any significant differences, $F(1, 8) = 0.305$, $p = 0.596$.

Figure 14a shows that the effects of a change in pitch dynamics on the crossover frequency in the pitch axis were very similar to the effects of a change in roll dynamics in the roll axis. The pitch crossover frequency in C2 was statistically significantly higher compared to the crossover frequency in C1, $t(8) = 7.169$, $p < 0.001$. Similar to the roll axis, there was a significant interaction between the axis of the changing dynamics and the initial and final crossover frequencies, $F(2, 16) = 81.114$, $p < 0.001$. The initial and final crossover frequencies were statistically significantly different for a change in roll dynamics only, $F(1, 8) = 11.229$, $p = 0.010$; for a change in pitch dynamics only, $F(1, 8) = 46.594$, $p < 0.001$; and for a combined change in roll and pitch dynamics, $F(1, 8) = 79.536$, $p < 0.001$. In the conditions with changing pitch dynamics, the final pitch crossover frequency was equal to the crossover frequency in C2. In the conditions with a change in roll dynamics only, the final crossover frequency was equal to the crossover frequency in C1 but significantly lower than the initial value, indicating a possible cross-coupling effect. No significant differences were introduced by the maximum rate of change, $F(1, 8) = 1.265$, $p = 0.293$.

The crossover frequency in the pitch axis was significantly higher than in the roll axis (comparing Figs. 13a, 14a), $F(1, 8) = 11.572$, $p = 0.009$.

For the phase margins in the roll and pitch axes, opposite trends were observed compared to the crossover frequencies. The roll-axis phase margin in condition C2 was statistically significantly lower compared to the phase margin in C1, $t(8) = 21.664$, $p < 0.001$ (Fig. 13b). A statistically significant interaction was found between the axis of the dynamics change and the initial and final phase margins in the conditions with time-varying dynamics, $F(2, 16) = 583.931$, $p < 0.001$. A significant lower value for the final roll phase margin than the initial phase margin was found in conditions with a change in roll dynamics only, $F(1, 8) = 386.723$, $p < 0.001$, and in conditions with a change in both roll and pitch dynamics, $F(1, 8) = 595.941$, $p < 0.001$. In these conditions, the final phase margin was equal to the phase margin in C2. In the conditions with a change in pitch dynamics only, a statistically significant higher final than initial phase margin was found, $F(1, 8) = 23.200$, $p = 0.001$, again indicating a possible cross-coupling effect. The maximum rate of change did not introduce any significant differences, $F(1,8) = 0.046$, $p = 0.836$.

Figure 14b indicates that the pitch phase margin in condition C2 was lower compared to condition C1, a statistically significant ef-

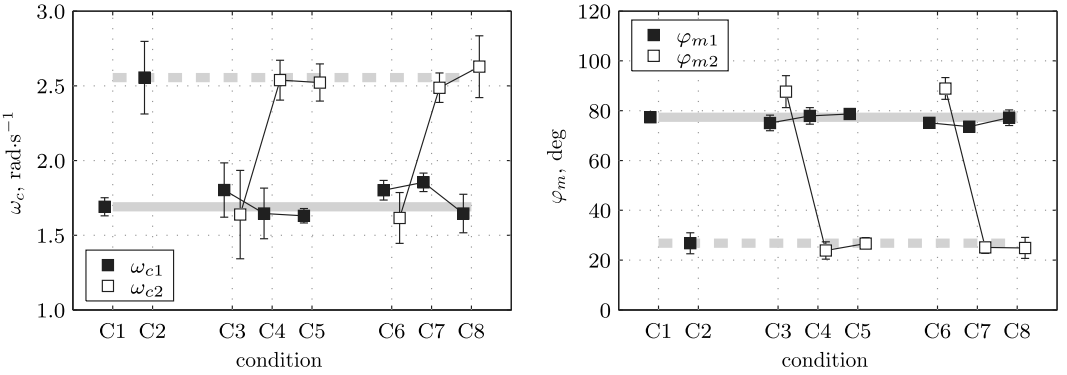

a) Pitch crossover frequency **b) Pitch phase margin**

Fig. 14 Pitch-axis crossover frequencies and phase margins.

fect $t(8) = 21.001$, $p < 0.001$. In the conditions with time-varying dynamics, a statistically significant interaction was found between the axis of the dynamics change and the initial and final phase margins, $F(2, 16) = 428.857$, $p < 0.001$. The final pitch phase margin was statistically significantly higher than the initial phase margin in the conditions with a change in roll dynamics only, $F(1, 8) = 48.339$, $p < 0.001$, and again, significantly lower and equal to the value in C2 in the conditions with a change pitch dynamics only, $F(1, 8) = 1377.695$, $p < 0.001$, and a change in both roll and pitch dynamics, $F(1, 8) = 448.961$, $p < 0.001$. The maximum rate of change did not introduce any significant differences, $F(1, 8) = 1.082$, $p = 0.329$.

Comparing the phase margins between the roll and pitch axes (Fig. 13b compared to Fig. 14b) revealed a statistically significant interaction between the axis of the changing controlled dynamics and the initial and final phase margins, $F(1, 8) = 10.802$, $p = 0.011$. The initial phase margin φ_{m1} was not statistically significantly different between the two axes, $F(1, 8) = 0.387$, $p = 0.551$, but the final phase margin φ_{m2} was significantly higher in the pitch axis compared to the roll axis, $F(1, 8) = 10.953$, $p = 0.011$.

VI. Discussion

A parameter estimation technique based on MLE was used to estimate the parameters of a pilot model with time-dependent sigmoid functions to characterize time-varying pilot control behavior in a roll–pitch control task. Several assumptions were made with respect to the time-varying pilot model.

The first assumption was that only the pilot equalization, defined by the visual gain and visual lead time constant, varied over time. The remaining parameters of the model, the visual time delay, neuromuscular damping, and neuromuscular frequency, were assumed to remain constant over time. This assumption was necessary to reduce the number of free parameters to be estimated by MLE, increasing the chance of finding a global optimum parameter set. Previous research showed that pilots mainly adapt their equalization dynamics when controlling the variation of controlled dynamics used in this study [13,14]. The assumption was validated by comparing constant pilot control behavior between two reference conditions with constant controlled dynamics, C1 and C2. The controlled dynamics in these conditions were the same as the initial and final controlled dynamics in conditions C3–C8. Comparing the estimated pilot model parameters between C1 and C2 showed that indeed only the visual gain and lead time constant were significantly different between the two conditions.

The second assumption was that the parameter function used for the time-varying pilot model parameters was equivalent to the parameter function used to vary the controlled dynamics over time, that is, a sigmoid function. By inspecting the time-domain data, this proved to be a valid assumption. However, when little is known about the characteristics of the time-varying controlled dynamics, the selection of the most appropriate parameter function to describe time variations in pilot model parameters might prove to be difficult. It requires incorporating available knowledge of the time-varying aspect of the controlled dynamics and careful inspection of the measured data. In practice, the complexity of the function will depend on many variables, such as the overshoot and settling time of the transient response. Care should be taken that not too many additional parameters are introduced by the parameter function because this can lead to an overparameterized pilot model, resulting in less accurate parameter estimates. Furthermore, it will be more difficult to find a global optimum parameter set because overparameterization increases the number of local optimum sets.

The final assumption was the introduction of an equivalent time of maximum rate of change M and maximum rate of change G for both parameter functions in the pilot model. This means that the time-varying parameters of the model changed at the same time and with the same maximum rate, with only their initial and final values being different. This reduces the number of parameters to be estimated, again resulting in more accurate parameter estimates. However, this assumption may not hold for all applications and must be considered in conjunction with the selection of the parameter function type.

To validate the accuracy of the pilot model, the VAF was calculated for the roll and pitch control signals. The VAF was generally around 70 and 82% for the roll and pitch axes, respectively. These values are slightly lower compared to values found in single-axis experiments [14]. This was an expected result because, in multi-axis control tasks, pilots' attention needs to be distributed between the two axes, resulting in higher levels of pilot remnant. The higher VAF for the pitch axis indicates that pilot control behavior was more linear in the pitch axis (that is, remnant levels were lower) compared to the roll axis. This could be due to the fact that a pitch error is more visible than a roll error due to the nature of the PFD used in the experiment (a roll disturbance is depicted by an angle deviation, whereas a pitch disturbance is depicted by a vertical displacement) or simply the fact that pilots paid more attention to pitch rather than roll.

Furthermore, as hypothesized in Sec. IV.B, the pilot model VAF for the double-integrator-like dynamics H_{c2} was higher compared to the pilot model VAF for the single-integrator-like dynamics H_{c1}. This was also found in previous experiments [22]. Finally, for the conditions with time-varying aircraft dynamics (C3–C8), a constant pilot model with five parameters $H_p(s)$ was identified in addition to the time-varying pilot model with nine parameters $H_p(s, t)$, to verify if that the addition of time-dependent sigmoid functions provides a higher overall model accuracy. This was indeed the case; for all conditions with time-varying aircraft dynamics, the VAF of the time-varying pilot model was significantly higher than the VAF of the constant model. The difference in VAF was greater in the pitch axis (approximately 7%) compared to the roll axis (approximately 3%).

The accuracy of the MLE procedure for the estimation of the parameters of a pilot model with time-dependent sigmoid functions was analyzed in a Monte Carlo analysis before the start of the experiment. This analysis showed that the final values of the sigmoid functions and the maximum rate of change have the highest bias and variance and that bias and variance increase when pilot remnant intensity increases. The lower accuracy of the maximum rate of change can be explained by the fact that this parameter is affected by data from a small time window only. In addition, the sigmoid function is a step function for maximum rates of change of approximately 10 to infinity (Sec. II.B), that is, virtually the same parameter optimization results will be obtained for $10 \leq G \leq \infty$.

The independent variables, the changing aircraft dynamics in the roll and pitch axes as well as the maximum rate of change of the dynamics, introduced significant differences in pilot control behavior. Mainly the pilot model parameters defining the time-dependent sigmoid functions were significantly affected. The main effect occurred in the axis of the changing controlled dynamics. However, significant effects were also found in the axis other than the axis of the changing controlled dynamics. This indicates that some cross coupling in pilot control behavior between the two axes is present and might warrant the addition of a cross-coupling path in a pilot model predicting multi-axis control behavior, even when the controlled dynamics in the two axis are not coupled.

Comparing the results across conditions between the roll and pitch axes, it was found that performance is higher and control activity is lower in the pitch axis. In addition, the average initial visual gain, final visual lead time constant, time delay, and neuromuscular frequency were all significantly higher for the pitch axis, whereas the neuromuscular damping was significantly lower. This also holds for the conditions with constant controlled dynamics. Note that the forcing functions were equivalent in both controlled axes, indicating that these effects were likely caused by differences in display or joystick characteristics between the two axes, differences in human perception and control processes between the two axes, or differential allocation of attention [3].

Most studies on pilot control behavior use single-axis control tasks and constant task variables such as the controlled dynamics. This reduces the applicability of the results from these studies to real piloting tasks because these are often performed in multiple axes at the same time and are not constant over time. In this paper, time-varying pilot control behavior was accurately identified using data from a multi-axis control task, further expanding the scope of pilot control behavior research. Further research is required to investigate

the use of different types of parameter functions to allow for more complex parameter variations in time. In addition, time variations in parameters other than the pilot equalization, such as time-varying perceptual time delays, should be investigated. Finally, a better way of identifying time variations in pilot model parameters might be to use methods such as the recursive least-squares method that do not require the prior definition of a specific parameter function [24]. However, more research is needed to determine the performance of these methods when applied to human operator data.

VII. Conclusions

An experiment was conducted with nine general aviation pilots who performed a roll–pitch control task with time-varying controlled dynamics. In eight experimental conditions, the axis containing the time-varying controlled dynamics and the maximum rate of change of the dynamics were varied. A maximum likelihood estimation (MLE) method was used to estimate the parameters of a pilot model with time-dependent sigmoid functions to characterize time-varying human control behavior in each condition. The main conclusions of this study are as follows:

1) Pilot control behavior in both the roll and pitch axes was significantly affected by the time-varying controlled dynamics and by the maximum rate of change of the dynamics. The main effect was found in the controlled axis that contained the time-varying controlled dynamics. However, significant effects were also found in the opposite axis, suggesting that cross coupling exists between pilot control behavior in the roll and pitch axes.

2) When the controlled dynamics in the pilot–vehicle crossover-frequency range changed from single-integrator to double-integrator dynamics, pilot gains decreased and visual lead generation increased. Pilot latencies and neuromuscular dynamics remained approximately constant.

3) Even though equivalent forcing functions were used in both axes of control, pilot performance was higher and control activity was lower in the pitch axis compared to the roll axis. This pattern was also reflected by significantly different pilot control behavior in both axes.

4) Overall, the MLE method was able to estimate most parameters of the time-varying pilot model accurately. The model parameters specifying the maximum rate of change of pilot control behavior and the pilot visual gain and lead time constant after the controlled dynamics change had the lowest estimation accuracy.

References

[1] Hess, R. A., "Modeling Pilot Control Behavior with Sudden Changes in Vehicle Dynamics," *Journal of Aircraft*, Vol. 39, No. 1, Sept.–Oct. 2009, pp. 1584–1592. doi:10.2514/1.41215

[2] Fletcher, J. W., Lusardi, J., Mansur, M., Moralis, E., and Robinson, D., "UH-60M Upgrade Fly-by- Wire Flight Control Risk Reduction Using the RASCAL JUH-60A In-Flight Simulator," *AHS 64th Annual Forum*, American Helicopter Society International SKU-64-2008-000330, Montreal, April–May 2008.

[3] Levison, W. H., "Two-Dimensional Manual Control Systems," *2nd Annual NASA-University Conference on Manual Control*, American Helicopter Soc. (AHS) International, Cambridge, MA, Feb.–March 1966, pp. 159–180.

[4] Chernikoff, R., Duey, J. W., and Taylor, F. V., "Two-Dimensional Tracking with Identical and Different Control Dynamics in Each Coordinate," *Journal of Experimental Psychology*, Vol. 60, No. 1, 1960, pp. 318–322. doi:10.1037/h0042961

[5] Duey, J., and Chernikoff, R., "The Use of Quickening in One Coordinate of a Two-Dimensional Tracking System," *Transactions on Human Factors in Electronics*, Vol. 1, No. 1, 1960, pp. 21–24. doi:10.1109/THFE2.1960.4503261.

[6] Todosiev, E. P., Rose, R. E., and Summers, L. G., "Human Performance in Single- and Two-Axis Tracking Systems," *2nd Annual NASA-University Conference on Manual Control*, American Helicopter Soc. (AHS) International, Cambridge, MA, Feb.– March 1966, pp. 143–158.

[7] Hess, R. A., "Modeling Human Pilot Adaptation to Flight Control Anomalies and Changing Task Demands," *Journal of Guidance, Control, and Dynamics*, advance online publication, June 2015. doi:10.2514/1.G001303.

[8] McRuer, D. T., Graham, D., Krendel, E. S., and Reisener, W., "Human Pilot Dynamics in Compensatory Systems: Theory, Models and Experiments with Controlled Element and Forcing Function Variations," U.S. Air Force Flight Dynamics Lab., TR AFFDL-TR-65-15, Wright Patterson AFB, OH, 1965.

[9] Stapleford, R. L., McRuer, D. T., and Magdaleno, R., "Pilot Describing Function Measurements in a Multiloop Task," *IEEE Transactions on Human Factors in Electronics*, Vol. 8, No. 2, 1967, pp. 113–125. doi:10.1109/THFE.1967.233628

[10] van Lunteren, A., "Identification of Human Operator Describing Function Models with One or Two Inputs in Closed Loop Systems," Ph. D. Dissertation, Faculty of Aerospace Engineering, Delft Univ. of Technology, Delft, The Netherlands, 1979.

[11] van der Vaart, J. C., "Modelling of Perception and Action in Compensatory Manual Control Tasks," Ph.D. Dissertation, Faculty of Aerospace Engineering, Delft Univ. of Technology, Delft, The Netherlands, 1992.

[12] Zaal, P. M. T., Pool, D. M., van Paassen, M. M., and Mulder, M., "Comparing Multimodal Pilot Pitch Control Behavior Between Simulated and Real Flight," *AIAA Modeling and Simulation Technologies Conference*, AIAA Paper 2011-6475, Aug. 2011. doi:10.2514/6.2011-6475.

[13] Breur, S. W., Pool, D. M., van Paassen, M. M., and Mulder, M., "Effects of Displayed Error Scaling in Compensatory Roll-Axis Tracking Tasks," *AIAA Guidance, Navigation, and Control Conference and Exhibit*, AIAA Paper 2010-8091, Aug. 2010. doi:10.2514/6.2010-8091.

[14] Zollner, H. G. H., Pool, D. M., Damveld, H. J., van Paassen, M. M., and Mulder, M., "The Effects of Controlled Element Break Frequency on Pilot Dynamics During Compensatory Target-Following," *AIAA Guidance, Navigation, and Control Conference and Exhibit*, AIAA Paper 2010-8092, Aug. 2010. doi:10.2514/6.2010-8092.

[15] Groot, T., Damveld, H. J., Mulder, M., and van Paassen, M. M., "Effects of Aeroelasticity on the Pilot's Psychomotor Behavior," *AIAA Atmospheric Flight Mechanics Conference and Exhibit*, AIAA Paper 2006-6494, Aug. 2006. doi:10.2514/6.2006-6494.

[16] Stapleford, R. L., Peters, R. A., and Alex, F. R., "Experiments and a Model for Pilot Dynamics with Visual and Motion Inputs," NASA CR-1325, 1969.

[17] Nieuwenhuizen, F. M., Zaal, P. M. T., Mulder, M., van Paassen, M. M., and Mulder, J. A., "Modeling Human Multichannel Perception and Control Using Linear Time-Invariant Models," *Journal of Guidance, Control, and Dynamics*, Vol. 31, No. 4, July–Aug. 2008, pp. 999–1013. doi:10.2514/1.32307

[18] Zaal, P. M. T., Pool, D. M., Chu, Q. P., van Paassen, M. M., Mulder, M., and Mulder, J. A., "Modeling Human Multimodal Perception and Control Using Genetic Maximum Likelihood Estimation," *Journal of Guidance, Control, and Dynamics*, Vol. 32, No. 4, July–Aug. 2009, pp. 1089–1099. doi:10.2514/1.42843

[19] Thompson, P. M., Klyde, D. H., and Brenner, M. J., "Wavelet-Based Time-Varying Human Operator Models," *AIAA Atmospheric Flight Mechanics Conference and Exhibit*, AIAA Paper 2001-4009, Aug. 2001, doi:10.2514/6.2001-4009.

[20] Thompson, P. M., and Klyde, D. H., "Exploration of the Properties of Analytic Wavelets for Systems Analysis," *AIAA Atmospheric Flight Mechanics Conference and Exhibit*, AIAA Paper 2002-4707, Aug. 2002. doi:10.2514/6.2002-4707.

[21] Thompson, P. M., Klyde, D. H., Bachelder, E. N., Rosenthal, T. J., and Brenner, M. J., "Development of Wavelet-Based Techniques for Detecting Loss of Control," *AIAA Atmospheric Flight Mechanics Conference and Exhibit*, AIAA Paper 2004-5064, Aug. 2004. doi:10.2514/6.2004-5064.

[22] Pool, D. M., Zaal, P. M. T., Damveld, H. J., van Paassen, M. M., van der Vaart, J. C., and Mulder, M., "Modeling Wide-Frequency-Range Pilot Equalization for Control of Aircraft Pitch Dynamics," *Journal of Guidance, Control, and Dynamics*, Vol. 34, No. 1, Sept.–Oct. 2011, pp. 1529–1542. doi:10.2514/1.53315

[23] Loftus, G. R., and Masson, M. E. J., "Using Confidence Intervals in Within-Subject Designs," *Psychonomic Bulletin and Review*, Vol. 1, No. 4, 1994, pp. 476–490. doi:10.3758/BF03210951

[24] Olivari, M., Nieuwenhuizen, F. M., Bülthoff, H. H., and Pollini, L., "Identifying Time-Varying Neuromuscular Response: Experimental Evaluation of a RLS-Based Algorithm," *AIAA Modeling and Simulation Technologies Conference*, AIAA Paper 2015-0658, Jan. 2015. doi:10.2514/6.2015-0658